ELSEVIER

Biomaterials 19 (1998) 717–724

Biomaterials

The effect of morphology variety of EVAL membranes on the behavior of myoblasts in vitro

Tai-Horng Young[a,*], Chun-Hsu Yao[a], Jui-Sheng Sun[b], Chao-Ping Lai[c], Leo-Wang Chen[c]

[a] *Center for Biomedical Engineering, College of Medicine, National Taiwan University, Taipei, Taiwan, Republic of China*
[b] *Department of Orthopaedic surgery, National Taiwan University Hospital, Taipei, Taiwan, Republic of China*
[c] *Department of Chemical Engineering, College of Engineering, National Taiwan University, Taipei, Taiwan, Republic of China*

Received 1 April 1997; accepted 10 September 1997

Abstract

Not only the surface morphology but also the surface chemistry can be changed during the fabrication of biomaterials. Therefore, the result of a biocompatibility test of one material may alter to a great extent, dependent on the fabrication process. In this paper, the in vitro interaction of myoblasts and EVAL membranes with different surface properties was investigated. It was observed that moderate contact angle and porous structure are favourable for the cell adhesion and growth. However, cell adhesion and growth were decreased on a porous structure with particulate morphology and higher contact angle.

Keywords: EVAL membranes; Myoblasts; Cell adhesion; Cell growth; Surface properties

1. Introduction

Recently, many techniques have been used to combine the membrane technology with biological cells to treat a specific disease, such as artificial pancreas [1–4] and membrane-guided bone regeneration [5, 6]. Much research has been explored in the studies of the biocompatibility of biomaterials [7–14]. However, the mechanism of cell adhesion and growth on different kinds of biomaterials is still not well established. This is due to the fact that it is difficult to attribute the difference of cell behaviour to the biomaterials themselves or other factors such as wettability, porosity, charge and roughness. In this study, we circumvented this problem by using one material, ethylene vinyl alcohol (EVAL), and evaluated the adhesion and growth of cells on the different structure of EVAL membranes.

Membranes are generally prepared by the phase inversion method [15]. In this process, a casting solution consisting of polymer and solvent inverts into a polymer network or gel to form the membrane. There are two kinds of phase inversion process: dry process or wet processes. In dry processes, a membrane is formed by complete evaporation of the solvent. In wet processes, the casting solution is immersed into a non-solvent coagulation bath. Interchange of solvent and non-solvent causes the casting solution to go through a phase transition to form a membrane.

The wet process involves two different types of phase transition [16]: solidification and liquid–liquid demixing (Fig. 1). When the viscosity of the polymer solution increases to a certain assumed value, the motion of polymer chains will be limited and the system can be regarded as a solid to fix the membrane structure. In liquid–liquid demixing, the completely miscible solution crosses the binodal boundary to enter the two-phase region. When a homogeneous solution becomes thermodynamically unstable, the solution can divide into two liquid phases of different composition to decrease its free energy of mixing. The two liquid phases reach the thermodynamic equilibrium and can be connected by the tie line in the phase diagram. If the polymer concentration of the phase transition is larger than the critical point, a nucleus of the polymer-poor phase that forms the pore, then a polymer-rich phase surrounds the pore. If the polymer concentration of the phase transition is smaller than the critical point, the polymer-rich phase separates as

* Corresponding author.

0142-9612/98/$19.00
PII S0142-9612(98)00187-7

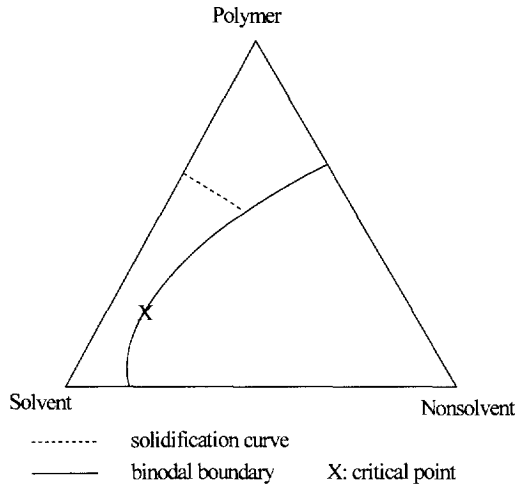

Fig. 1. Typical ternary phase diagram of polymer–solvent–non-solvent.

a nucleus of a particle rather than the formation of a nucleus of polymer-poor phase.

The phase diagram is the description of an equilibrium state. In membrane formation, the membrane structure is mainly governed by the composition variation of the casting solution at the instant of phase transition [17]. Three types of membranes can form.

(1) A dense structure is formed when the composition variation path enters the solidification region directly.

(2) If the composition variation path crosses the binodal boundary above the critical point, a porous structure is formed. The polymer is then served as a continuous matrix in the membrane.

(3) A particle-bonded structure is formed if the composition variation path crosses the binodal boundary below the critical point. The polymer acts as a discontinuous matrix in the membrane.

The recent progress in biomaterials has raised the advancement in orthopaedic surgery. The bone and soft tissues present around the biomaterials may be adversely affected by the cell-material interaction after implantation. Based on the clinical experience, it is impossible for bone defect healing when the muscle tissue around the bone defect is seriously hurt. This can be ascribed to the fact that the blood supply of bone is from muscle tissue. Therefore, after implantation of biomaterials, the skeletal muscles are also exposed to the effect of device-related factors. There were many discussions in the literature describing the effects of biomaterials on bone tissue, but few references described the effect of the morphology of material surface on the skeletal muscles [7, 18]. Therefore, following the above membrane formation mechanism, the adhesion and growth of myoblasts on a series of well-characterized EVAL membrane were presented to study cell behaviour on the same material, but with different morphology in vitro.

2. Materials and methods

2.1. Materials

EVAL copolymer of 56 mol% of vinyl alcohol monomeric units was obtained using the previously reported techniques [19]. In this study, de-ionized and ultrafiltrated water were used. Other reagents were of chemical reagent grade and were used without further purification.

2.2. Membrane preparation

EVAL copolymer was dissolved in dimethyl sulphoxide (DMSO) to form a 25 wt% polymer solution at 60°C. The solution was kept at 25°C for 24 h and then was spread on a glass plate in a uniform thickness of 175 μm at 25°C to prepare membranes.

EVAL membranes were identified by the letters A, B and C in Table 1. Membrane A was prepared by evaporating DMSO at 70°C. Membranes B and C were prepared by immersing the casting solution immediately (no evaporation step) into a non-solvent bath. The non-solvent bath for membrane B was water maintained at 60°C. The non-solvent bath for membrane C was a DMSO/water mixture containing 80 wt% DMSO maintained at 25°C. After the evaporation and precipitation were completed (*ca* 1 day), the membranes were removed from the glass plate and kept in a water bath at 25°C for 24 h.

2.3. Membrane characterization

The morphology of the membranes was examined on freeze-dried samples using a scanning electron microscope (SEM). Contact angles were measured at 25°C in water using a reverse air-bubble apparatus (CA-D, Kyowa Scientific Co.). The porosity of membranes was measured on freeze-dried samples by mercury intrusion porosimetry (Micrometrics Autopore II-9220). The intrusion volume was recorded for various pressures ranging from 0 to 50,000 psi.

Table 1
Characteristics of EVAL membranes

Membrane	Phase inversion	Morphology	Contact angle (deg)	Porosity
A	Dry	Dense	44.2 ± 1.6	0.00[a]
B	Wet	Porous	34.5[b] ± 3.0	0.60[b] ± 0.11
C	Wet	Particles-bonded	55.0[b] ± 1.6	0.64[b] ± 0.05

Sample numbers $n = 6$.

[a] The smallest pore that can be measured in the porosimetry is 3 nm.

[b] These data show a significant difference of membrane properties ($P < 0.05$) compared with membrane A.

2.4. Cell culture

Primary culture of Wistar rat myoblasts were used in this study. Myoblast cells were isolated from male Wistar rats (250–350 g) by enzymatic digestion technique following the method of Bischoff [20]. The culture media used was Dulbecco's modified Eagle's medium (MEM) supplemented with 10% foetal calf serum (Gibco-RBL Life Technologies, Paisley, U.K.) and 1% antibiotics (penicillin G sodium 100 U ml^{-1} streptomycin 100 U ml^{-1}, Gibco-RBL Life Technologies, Paisley, U.K.).

EVAL membranes were mounted in six-welled tissue culture polystyrene plates (Corning, New York, U.S.A.) by surgical adhesive CYNAL-5 (Nycomed Ingenor, France). The mounted membranes were rinsed extensively with distilled water and subsequently sterilized under ultraviolet light overnight. Then 3 ml of cell suspension seeded on to the surface of membrane (2.25×10^5 cells per well). Cell cultures were maintained in a humidified atmosphere with 5% CO_2 at 37°C.

After 4 h incubation, the membrane surface was washed with phosphate buffer solution (PBS) twice to remove cell debris being present in the medium. Adhering cells were detached with tryspin, stained with trypan blue to make sure the cell viability and counted using a Neubauer counting-chamber under the inverted microscope [7]. The myoblasts adhesion to a membrane was expressed as the percentage of the cells adhering to the tissue culture polystyrene. Cell growth on the membrane was carried out for 2, 4 and 7 days in the same way as the cell adhesion.

For morphological observation, the cells adhering to the membrane were washed with PBS and then fixed with 2.5% glutaraldehyde in PBS for 1 h at 4°C. After thorough washing with PBS, the cells were dehydrated by graded ethanol changes and then the critical point dried. The membranes were then gold sputtered in vacuum and examined by SEM.

2.5. Data analysis

All experiments were repeated six times ($n = 6$) and results are expressed as mean ± SEM (standard error of mean). The differences between various membranes were evaluated by using Student's t-test. Significance was assessed at the $P < 0.05$ level of confidence.

3. Results and discussion

3.1. Morphology of membranes

Macroscopically, membrane A was transparent, whilst B and C appeared opaque. The microstructure of EVAL membranes was analysed qualitatively by SEM. Membrane A showed fairly dense and smooth structure (Fig. 2a). The membrane formation mechanism is described in Fig. 3. Point I was the initial composition of the casting solution on the solvent–polymer line. The composition variation path of membrane A followed the line I-A by complete evaporation of the solvent and a dense structure was formed.

Membrane B coagulated in a water bath at 60°C showed a heterogeneous morphology with pores either superficial or open to the interior (Fig. 2b). If the membrane was prepared by using water at 25°C as a coagulation agent, it showed a dense skin with a porous sublayer (SEM pictures were presented in [16]: Fig. 2). Such a complex behaviour is thought to be due to the following [16]. The interaction between DMSO and water is strong, DMSO in the casting solution dissolves rapidly into the water coagulation bath at the moment the casting solution and water come into contact. However, relatively little water diffuses into the casting solution since it is a non-solvent for EVAL copolymer. As shown in Fig. 3, the composition variation path entered the solidification region directly following the line I-B′ during the membrane formation at a 25°C water bath. The role of water changed from a strong non-solvent to a weak one at 60°C [19] so the diffusion of water into the casting solution increased. In addition, since mixing DMSO and water was exothermic, the DMSO outflow decreased by increasing the temperature of the coagulation bath. The outcome was the composition variation path of membrane B followed the line I-B through the binodal boundary to cause liquid–liquid phase separation to form a porous structure on the surface.

Membrane C, coagulated in a DMSO/water bath containing 80% DMSO, formed the constituent particles ranging from 0.2 to 0.5 μm (Fig. 2c). Adding solvent to the coagulation bath was similar to the coagulation bath at high temperatures, which could reduce the interaction between solvent and non-solvent mixture. The diffusion tendency of solvent into the coagulation was reduced, therefore, the composition variation path could reach the binodal boundary at a lower polymer concentration, even smaller than the critical solution concentration; see the line I-C in Fig. 3. Consequently, concentrated polymer droplets dispersed in a dilute polymer solution to form the particle-bonded structure.

3.2. Contact angles of membranes

Underwater contact angles are shown in Table 1. These data show a significant difference ($P < 0.05$) of membrane properties compared with the membrane A. Membrane B had the most hydrophilic surface with a contact angle of 34.5 ± 3.0° and membrane C was the most hydrophobic with a contact angle of 55.0 ± 1.6°. Membrane A, with a contact angle of 44.2 ± 1.6°, was between membranes B and C.

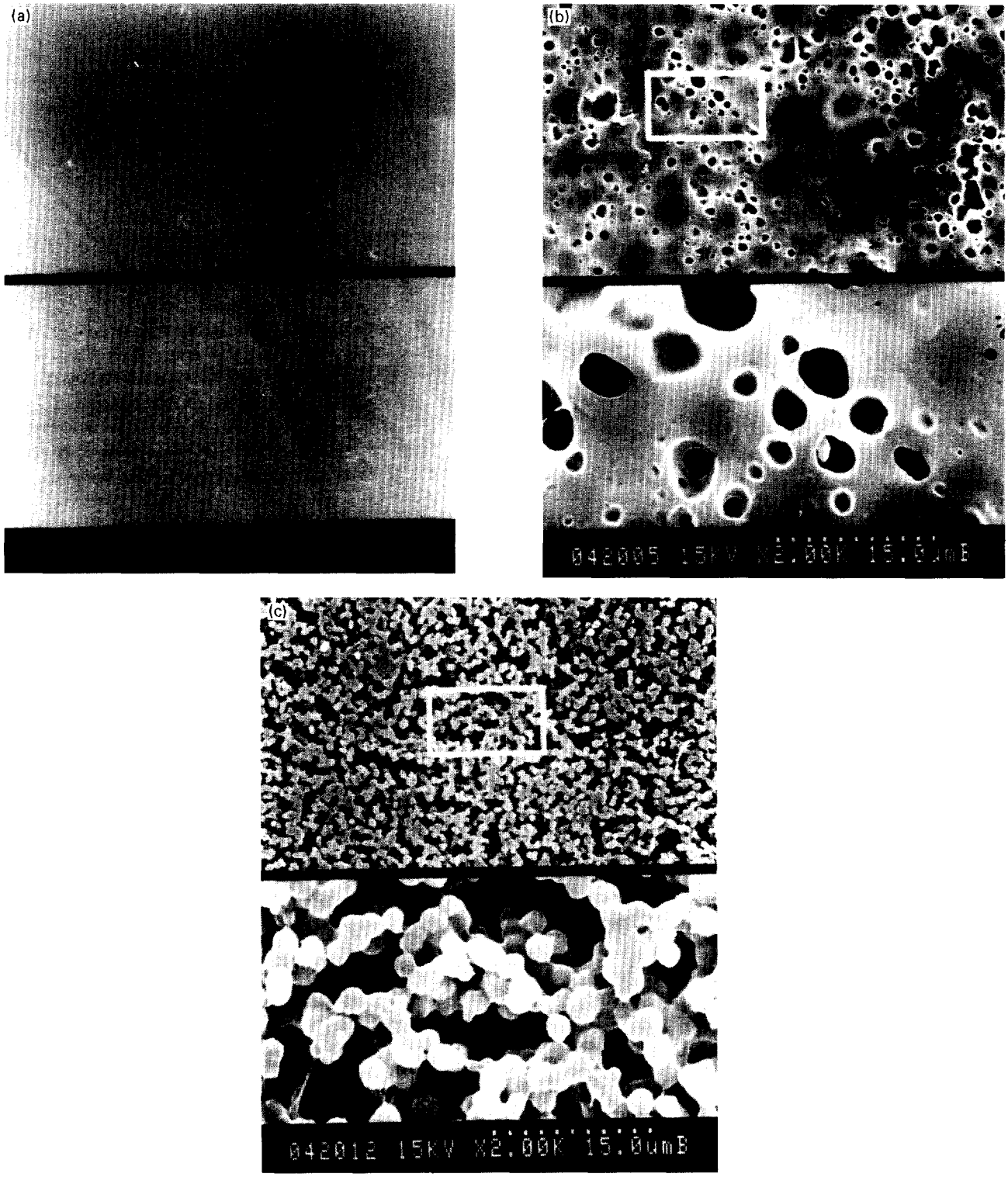

Fig. 2. SEM pictures of EVAL membranes: (a) A; (b) B and (c) C.

This reflected that the hydrophobic ethylene segments and the hydrophilic vinyl alcohol segments were selectively present at the surface in the course of preparation of the membrane. Although this is a relatively slow process in the case of rigid polymers, molecules in a solution state have the ability to rearrange and reorganize their surface structures. The contact angle of membrane B suggested that the hydrophilic components of EVAL molecules may migrate toward the surface at the moment that the casting solution and water came into contact.

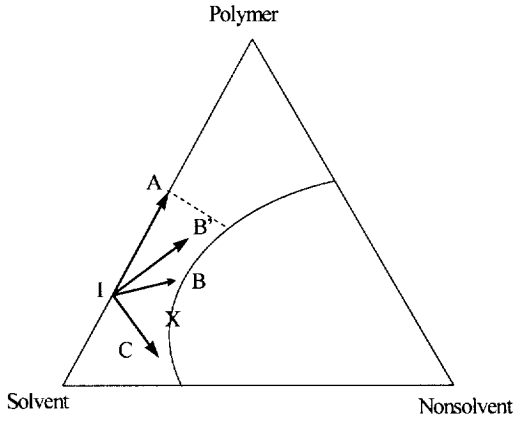

Fig. 3. Composition paths of EVAL membranes A (I-A), B (I-B) and C (I-C).

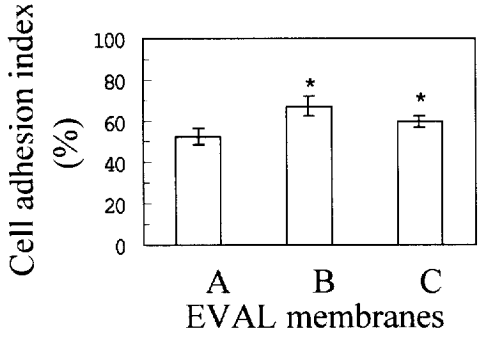

Fig. 4. Relative value of myoblasts adhesion on EVAL membranes after 4 h culture. Sample numbers $n = 6$. (*These data show a significant difference of cell adhesion ($P < 0.05$) compared to the membrane A.)

Membrane A formation occurred in a dry state, the surface was enriched with hydrophobic ethylene segments and hydroxyl groups were embedded into the deeper layer of the material. The spherical shape of EVAL molecules in membrane C might be the effect responsible for the highest contact angle. From a thermodynamic point of view, the spherical shape has the lowest surface energy. Therefore, every particle of membrane C minimized its surface polarity in the particle formation.

3.3. Cell adhesion

We expressed the results from the adhesion tests on the EVAL membranes as a percentage of the control (Fig. 4). It appeared that within 4 h, there was a significant difference ($P < 0.05$) of the cell adhesion on membranes B and C compared with membrane A (52% of the control). For membranes B and C, respectively, cell adhesion was significantly higher for membrane B when compared with C ($P < 0.05$). Approximately 67% of cells adhered on the most hydrophilic membrane B relative to the control. Less cells adhered on the most hydrophobic membrane C (60%). Despite the contact angle of membrane A being between that of membranes B and C, however, it showed a poor adhesion of myoblasts. The result was supported by the work of others. Wachem et al. [8] demonstrated that human endothelial cells adhered and spread preferably on moderately wettable polymers with a water contact angle of 35°. Lee and Lee [12] found the maximum adhesion of the Chinese hamster ovary cells appeared at around a water contact angle of 55°. A perfect relationship between cell adhesion and contact angle was not found. Therefore, the effect of contact angle probably only resulted in the limited correlation on cell adhesion.

Another important factor affecting cell adhesion is the surface morphology on which the cultured cells attach. For example, it is reasonable to hypothesize that the amount of cell adhesion would increase as the area of its contact with the surface increases. Therefore, the surface of membrane A which was very dense without any pore from SEM picture (Fig. 2a) showed the poorest cell adhesion. Membrane B with the most cell adhesion, besides the effect of hydrophilicity, was probably due to the porous structure. Comparing the bulk porosity of membranes B and C, there were no significant differences ($P > 0.05$) between them (Table 1). Therefore, it is reasonable to assume they have a similar surface area for cell adhesion. However, the polymer served as a continuous matrix in membrane B and the pore served as a continuous matrix in membrane C. In addition, the surface is concave on the pore of membrane B and the surface is convex on the particle of membrane C. Consequently, membrane C with less cell adhesion than B was probably due to the effects combined with hydrophobicity and particulate morphology, not their contact area, as indicated by the results of this work.

After cell contact surfaces, cells will alter their cell membrane and its morphology to stabilize the cell–material interface [14]. Cell morphology on the membranes was studied using SEM. There were observable differences among the morphologies of myoblast cells cultured on the various membranes at the same incubation time. Fig. 5 showed the SEM pictures of the myoblast cells grown on the EVAL membranes after 4 h culture. Cells on membrane B were completely flattened and well spread. Similarly, cells on membrane A were also spread. Although membrane C showed more adhesion of the myoblast cells than A, the SEM observation revealed that the cells were spread better on the membrane A than on the membrane C. The cells were not spread at all and remained spherical on membrane C. Obviously, cell adhesion might increase as the area of its contact with the substratum increases, however, it does not promise that cells can spread very well. Therefore, on membranes A and B better cell spreading was probably due to their moderate hydrophilicity.

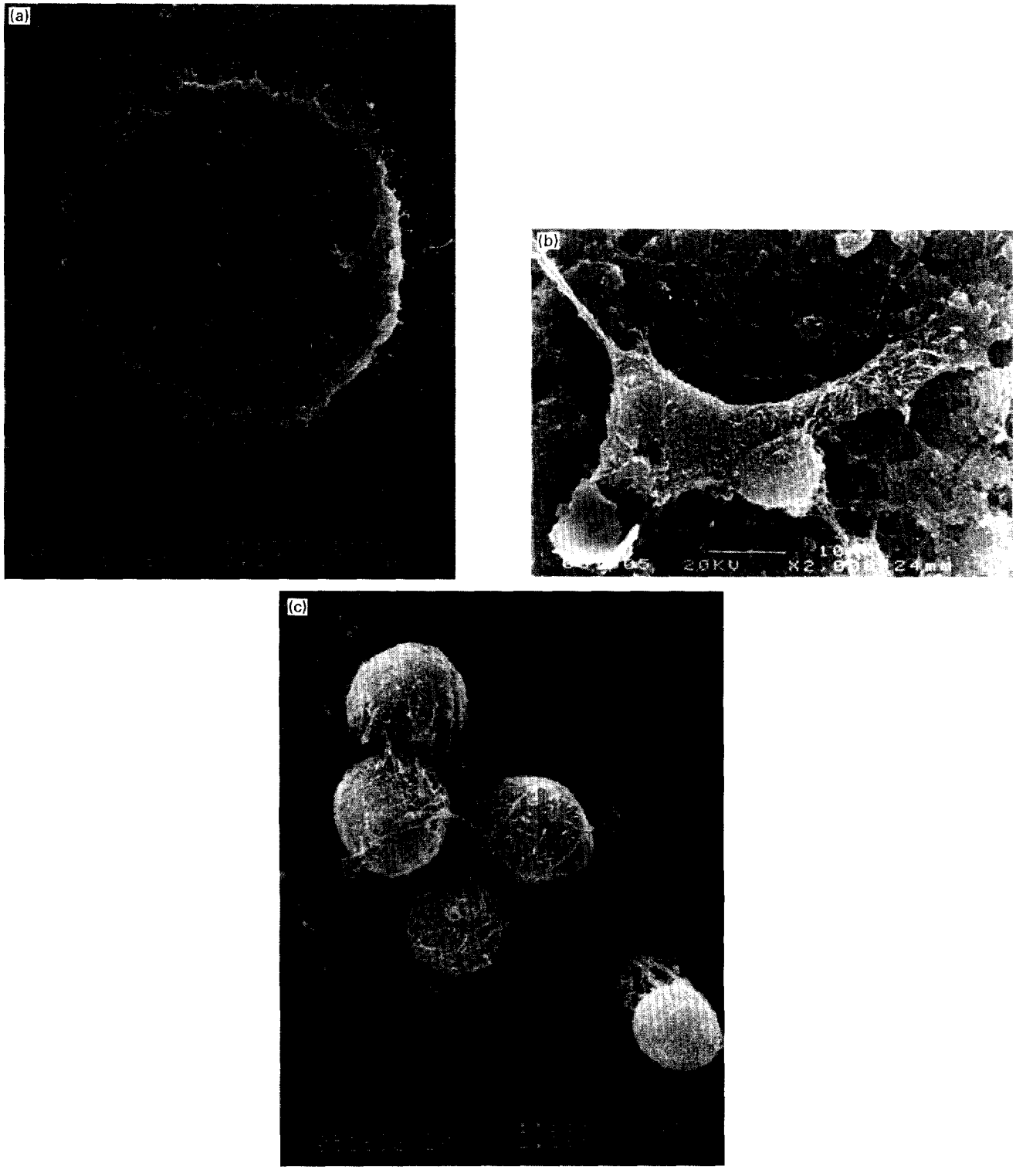

Fig. 5. SEM pictures of myoblasts adhered on EVAL membranes after 4 h culture. (a) membrane A: the cell constitutes the centrifugal growth of filopodia; (b) membrane B: the cell has almost completed adhesion and spreading; (c) membrane C: the cells remain spherical at points of contact with membrane C.

3.4. Cell growth

When cell adhesion was followed by progressive flattening of the cells, proliferation occurred. Fig. 6 showed the number of myoblast cells on the EVAL membranes after 2, 4 and 7 days culture. After 4 days culture cell numbers had increased 2–4-fold compared with those after 2 days culture. At 7 days a minor cell proliferation

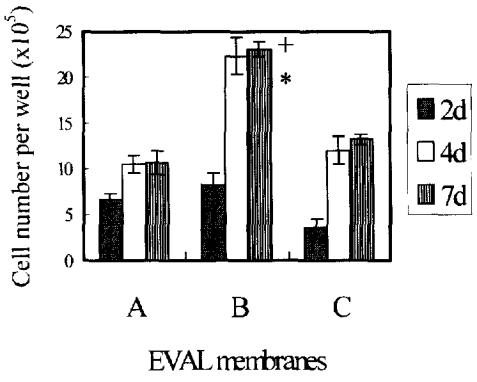

Fig. 6. The number of myoblasts on EVAL membranes after 2, 4 and 7 days culture. Sample numbers $n = 6$. (+This data show a significant difference ($P < 0.01$) between membrane A and B after 7 d culture. *This data show a significant difference ($P < 0.01$) between membrane C and B after 7 d culture.)

occurred on all the EVAL membranes compared with the preceding days. All the growth became relatively slow and the cell number did not change significantly.

The cell growth was similar to the cell adhesion; membrane B showed the highest cell number after 7 days culture ($P < 0.01$). Although membrane C showed more adhesion of the myoblast cells than A, the numbers of myoblast cells were similar between membranes A and C after 7 days culture ($P > 0.05$). The result can be ascribed to the fact that the cells were spread better on membrane A than on membrane C, therefore, there was no difference in the cell growth between membranes A and C.

The interactions of cells with solid substrates depend on many factors, such as wettability, porosity, chemistry, charge and rigidity. The results of increasing cell culture toward the porous surfaces in this study agreed with those of other works [8, 10, 12]. Although the particle-bonded surface had enough porosity, the cell behaviour on the particle-bonded surface was not good. It is possible that microparticulate morphology would not be beneficial to cell spreading. A thorough study of the effects of polymer surface properties on the biocompatibility will be followed by in vivo evaluation.

4. Conclusion

We prepared EVAL membranes with different structure by the phase inversion process and studied the adhesion and growth of myoblasts on the different structure of EVAL membranes. The major advantage is that different structures are effectively compared on the same material. The result clearly demonstrated that the hydrophilicity and the morphology of membrane were important factors for cell adhesion and growth. Therefore, it is difficult to compare the cell behaviour on different materials when the surface properties are not well defined.

Acknowledgement

The authors thank the National Science Council of the Republic of China for their financial support by project NSC 85-2331-B-002-181-M08.

References

[1] Lim F, Sun AM. Microencapsulated islets as bioartificial endocrine pancreas. Science 1980;210:908–10.
[2] Altman JJ, Houlbert A, Callard P, McMillan P, Solomon BA, Rosen J, Galetti PM. Long term plasma glucose normalization in experimental diabetic rats with macroencapsulated implants of benign human insulinomas. Diabetes 1986;35:625–33.
[3] Kessler L, Aprahamian M, Keipes M, Damge C, Pinget M, Poinsot D. Diffusion properties of an artificial membrane used for Langerhans islets encapsulation: an in vitro test. Biomaterials 1992;13:44–49.
[4] Young TH, Yao NK, Chang RF, Chen LW. Evaluation of asymmetric poly(vinyl alcohol) membranes for use in the artificial islets. Biomaterials 1996;17:2131–37.
[5] Caffesse RG, Nasjleti CE, Morrison EC, Sanchez R. Guided Tissue Regeneration: comparison of bioabsorbable membranes. Histologic and histometric study in dogs. J Periodontol 1994;65:583–91.
[6] Nyman R, Magnusson M, Sennerby L, Nyman S, Lundgren D. Membrane-guided bone regeneration. Segmental radius defects studied in the rabbit. Acta Orthop Scand 1995;66:169–73.
[7] Derker C, Greggs R, Duggan K, Stubbs J, Horwitz A. Adhesive multiplicity in the interaction of embroyonic fibroblasts and myoblasts with extracellular matrices. Cell Biol 1984;99: 1398–1404.
[8] van Wachem PB, Beugeling T, Feijen J, Bantjes A, Detmers JP, van Aken WG. Interaction of cultured human endothelial cells with polymeric surfaces of different wettabilities. Biomaterials 1985;6:403–8.
[9] Schakenraad JM, Busscher HJ, Wildevuur CHR, Arends J. The influence of substratum surface free energy on growth and spreading of human fibroblasts in the presence and absence of serum proteins. J Biomed Mater Res 1986;20:773–84.
[10] van Wachem PB, Hogt AH, Beugeling T, Feijen J, Bantjes A, Detmers JP, van Aken WG. Adhesion of cultured human endothelial cells onto methacrylate polymers with varying surface wettability and charge. Biomaterials 1987;8:323–28.
[11] Van Kooten TG, Schakenraad JM, van der Mei HC, Busscher HJ. Influence of substratum wettability on the strength of adhesion of human fibroblasts. Biomaterials 1992;13:897–904.
[12] Lee JH, Lee HB. A wettability gradient as a tool to study protein adsorption and cell adhesion on polymer surface. J Biomater Sci Polym Edn 1993;4:467–81.
[13] Lee JH, Jung HW, Kang IK, Lee HB. Cell behaviour on polymer surfaces with different functional groups. Biomaterials 1994;15: 705–11.
[14] Okano ZT, Yamada N, Okuhara M, Sakai H, Sakurai Y. Mechanism of cell detachment from temperature-modulated, hydrophilic-hydrophobic polymer surfaces. Biomaterials 1995;16: 297–303.

[15] Kesting RE. Synthetic polymeric membranes. New York: John Wiley and Sons, 1985.
[16] Young TH, Chen LW. A two step mechanism of diffusion controlled ethylene vinyl alcohol membrane formation. J Membrane Sci 1991;57:69–81.
[17] Young TH, Chen LW, Cheng LP. Membranes with a microparticulate morphology. Polymer 1996;37:1305–10.
[18] Sun JS, Tsuang YH, Yao CH, Liu HC, Lin FH, Hang YS. Effects of calcium phosphate bioceramics on skeletal muscle cells. J Biomed Mater Res 1997;34:227–34.
[19] Chen LW, Young TH. EVAL membranes for blood dialysis. Makromol Chem Macromol Symp 1990;33:183–99.
[20] Bischoff R. Enzymatic liberation of myogenic cells from adult rat muscle. Anat Rec 1974;180:645–62.